

See discussions, stats, and author profiles for this publication at: <https://www.researchgate.net/publication/6258677>

# Polyelectrolyte-Mediated Adsorption of Amelogenin Monomers and Nanospheres Forming Mono- or Multilayers

ARTICLE in BIOMACROMOLECULES · AUGUST 2007

Impact Factor: 5.75 · DOI: 10.1021/bm070088+ · Source: PubMed

CITATIONS

12

READS

28

## 4 AUTHORS:



**Csilla Gergely**

Université de Montpellier

148 PUBLICATIONS 1,872 CITATIONS

SEE PROFILE



**Balazs Szalontai**

Hungarian Academy of Sciences

56 PUBLICATIONS 1,070 CITATIONS

SEE PROFILE



**Janet Moradian-Oldak**

University of Southern California

138 PUBLICATIONS 4,468 CITATIONS

SEE PROFILE



**Frédéric Cuisinier**

Université de Montpellier

199 PUBLICATIONS 3,208 CITATIONS

SEE PROFILE

## Polyelectrolyte-Mediated Adsorption of Amelogenin Monomers and Nanospheres Forming Mono- or Multilayers

Csilla Gergely,<sup>\*,†</sup> Balázs Szalontai,<sup>‡</sup> Janet Moradian-Oldak,<sup>§</sup> and Frédéric J. G. Cuisinier<sup>||</sup>

*Groupe d'étude des semi-conducteurs, Université Montpellier II, Montpellier Cedex 5, France, Institute of Biophysics, Biological Research Center of the Hungarian Academy of Sciences, Szeged, Hungary, Center for Craniofacial Molecular Biology, University of Southern California, Los Angeles, California, and Faculté de Chirurgie Dentaire, Université Montpellier I, Montpellier Cedex 5, France*

*Received January 24, 2007; Revised Manuscript Received April 28, 2007*

We have applied optical waveguide lightmode spectroscopy combined with streaming potential measurements and Fourier-transformed infrared spectroscopy to investigate adsorption of amelogenin nanospheres onto polyelectrolytes. The long-term objective was to better understand the chemical nature of these assemblies and to gain further insight into the molecular mechanisms involved during self-assembly. It was found that monolayers of monomers and negatively charged nanospheres of a recombinant amelogenin (rM179) irreversibly adsorbed onto a positively charged polyelectrolyte multilayer films. On the basis of measurements performed at different temperatures, it was demonstrated that intermolecular interactions for the formation of nanospheres were not affected by their adsorption onto polyelectrolytes. Consecutive adsorption of nanospheres resulting in the formation of multilayer structures was possible by using cationic poly(L-lysine) as mediators. N-Acetyl-D-glucosamine (GlcNAc) did not disturb the nanosphere-assembled protein's structure, and it only affected the adsorption of monomeric amelogenin. Infrared spectroscopy of adsorbed amelogenin revealed conformational differences between the monomeric and assembled forms of rM179. While there was a considerable amount of  $\alpha$ -helices in the monomers,  $\beta$ -turn and  $\beta$ -sheet structures dominated the assembled proteins. Our work constitutes the first report on a structurally controlled in vitro buildup of an rM179 nanosphere monolayer-based matrix. Our data support the notion that amelogenin self-assembly is mostly driven by hydrophobic interactions and that amelogenin/PEM interactions are dominated by electrostatic forces. We suggest that similar forces can govern amelogenin interactions with non-amelogenins or the mineral phase during enamel biomineralization.

### Introduction

Amelogenins are the principle protein components of the developing enamel extracellular matrix<sup>1</sup> accounting for approximately 90% of all the proteins in the matrix.<sup>2,3</sup> The protein is enriched in hydrophobic amino acids such as Pro, Glu, and Leu. It has been shown that recombinant amelogenin molecules spontaneously self-assemble in solution to form monodispersed (polydispersity <15%) structures called nanospheres.<sup>4,5</sup> Dynamic light scattering (DLS), atomic force, and transmission electron microscopy revealed the formation of nanospheres of about 20–100 nm in diameter depending on the solution conditions.<sup>6</sup> The self-assembly process was sensitive to solution pH and temperature and it has been demonstrated to be hydrophobically driven.<sup>7,8</sup> Nanospheres were identified in histological sections of developing mouse molars as beaded rows surrounding the tiny enamel crystallites at the early stage of enamel formation.<sup>9</sup> For an insight to the emergence of amelogenin nanospheres as basic structural units and their comparison with structures in the developing enamel matrix, refer to Moradian-Oldak<sup>3</sup> and Moradian-Oldak and Goldberg.<sup>10</sup> Further DLS measurements were performed to report the size distribution of nanospheres

formed by a series of native and recombinant proteins.<sup>11</sup> Amelogenins lacking the carboxy-terminal formed larger nanospheres due to their further association through hydrophobic interactions and their binding affinity to apatite crystals was considerably lower compared to native amelogenins.<sup>11</sup>

Amelogenin sequences at both carboxyl- and amino-terminal regions across species are highly homologous suggesting that these regions play specific functional roles during matrix mediated enamel biomineralization. Studies on amelogenin proteolysis combined with mass spectrometry furnished information on the surface accessibility of conserved domains of amelogenin assemblies.<sup>6</sup> By applying a limited proteolysis approach, it has been demonstrated that regions at the N- and C-terminal of amelogenin are exposed on the surface of these nanospheres. The 17 N-terminal residues were protected from proteolysis suggesting their involvement in protein–protein interaction in nanosphere formation. Two domains, an amino-terminal (1–42 residues) and a carboxyl-terminal (157–173 residues), were identified as mediating amelogenin self-assembly.<sup>12</sup> Although the bulk of amelogenin is rich in hydrophobic amino acids, the C-terminal region is composed of a sequence of hydrophilic and charged amino-acids. Earlier studies revealed that amelogenins interact directly, via this charged C-terminal, with enamel apatite crystals.<sup>13,6</sup> Two-hybrid assay and surface plasmon resonance data support that the amelogenin amino-terminal self-assembly domain is essential for the assembly of an enamel extracellular organic matrix capable of directing mineral formation.<sup>14</sup>

\* Corresponding author. Address: Groupe d'étude des semi-conducteurs, Université Montpellier II, Place Eugène Bataillon, 34095 Montpellier Cedex 05, France. Tel: 33467143248. Fax: 33467143760. E-mail: gergely@ges.univ-montp2.fr.

† Université Montpellier II.

‡ Biological Research Center of the Hungarian Academy of Sciences.

§ University of Southern California.

|| Université Montpellier I.

Numerous *in vivo* and *in vitro* studies have collectively suggested that amelogenin self-assembly is a critical parameter for normal enamel formation (amelogenesis). For an updated review on mechanisms of enamel formation, see Moradian-Oldak and Paine.<sup>15</sup>

Supramolecular self-assembly of amelogenin nanospheres into nanochains and microribbons has also been demonstrated.<sup>16,17</sup> It has been proposed that amelogenin nanospheres provide the temporary scaffold for the oriented growth of enamel crystals during the early stage of enamel development.<sup>18,19</sup> A cooperative mechanism for amelogenin–mineral supramolecular co-assembly during enamel biomineralization has been also proposed.<sup>20,21</sup>

Protein adsorption on surfaces is a complex process, which is governed by the hydrophobicity and hydrophilicity of the surface,<sup>22</sup> but also the surface charge,<sup>23</sup> roughness,<sup>24</sup> and free energy.<sup>25,26</sup> A new type of tunable surface for controlling substrate chemistry is provided by the use of polyelectrolyte multilayers (PEM). PEM's are formed by alternating adsorption of polycations and polyanions in aqueous solution on a charged, solid surface.<sup>27</sup> Due to this layer-by-layer construction all PEM exhibit excess charges, alternatively positive and negative on their surfaces. These excess charges are the motor of their buildup, and also facilitate the adsorption of a great variety of compounds on the PEM surface. Thus, PEM's may offer convenient solutions for the problems encountered due to anchoring of proteins to bare surfaces. Direct adsorption of a protein onto a surface constitutes a physisorption that frequently induces loss of the functional activity and denaturing of the adsorbed protein. Numerous studies revealed that a underlying PEM coating can preserve the secondary structure of proteins<sup>28,29</sup> the helical structure of DNA,<sup>30</sup> or poly(L-lysine).<sup>31</sup> Studying protein adsorption on PEM's provides insight into the role of surface charges in protein adsorption processes, even though there is a major difference between adsorption on surfaces covered with water-soluble polyelectrolytes and on hard charged surfaces in general. The alternated adsorption of oppositely charged poly-ions at a solid/liquid interface constitutes a versatile and powerful assembling technique for supramolecular architectures.<sup>32</sup> Polyelectrolytes on surfaces extend loops and tails that are flexible and thus accommodate to the shapes of the protein molecules, but can also present advantages in adsorption of bigger structures like amelogenin nanospheres.

The aim of the present study was to describe the adsorption of recombinant mouse amelogenin (rM179) nanospheres on charged surfaces, and gain insight into the self-assembly process, when strong external constraints are applied on these nanostructures. We report results on the surface charges of recombinant mouse amelogenin nanospheres and their adsorption on previously modified surfaces: the substrates were coated by PEM's, formed by alternating physisorption of polystyrenesulfonate (PSS) and polyallylamine (PAH) on a precursor layer of polyethylenimine (PEI). The data obtained from streaming potential measurements and optical waveguide lightmode spectroscopy (OWLS) were the  $\zeta$  potential, thickness, refractive index, and the amount of the adsorbed material, which were used to characterize the *in situ* buildup of PEM's and adsorption of amelogenin protein (mono or multilayer). Furthermore, we seek to study the role of the nanosphere surface charges in amelogenin supramolecular assembly. These phenomena were studied with the help of different PEM film surfaces, combined with additional materials, like poly(L-lysine), N-acetyl-D-glucosamine to aid nanosphere assembly, and finally in monomeric form in the presence of acetonitrile.

Fourier-transformed infrared (FTIR) spectroscopy was employed to provide details on eventual structural rearrangements of the protein upon adsorption onto PEM. The results of these measurements point to considerable differences between monomeric and assembled amelogenin when adsorbed onto the charged surfaces of the polyelectrolyte multilayers.

## Experimental Section

**Materials.** 1. *Polyelectrolyte Solutions.* Anionic poly(sodium 4-styrenesulfonate) (PSS, MW = 60 000), cationic poly(allylamine hydrochloride) (PAH, MW = 70000), cationic poly(ethyleneimine) (PEI, 95%, MW = 60000), poly(L-lysine) (PLL, 90–94%, MW = 30 000–46 000), and N-acetyl-D-glucosamine, GlcNac (99%, MW=221.21) were purchased from Aldrich and Tris (hydroxymethylaminomethane) from Sigma. All the chemicals of commercial origin were used without further purification. All the buffer solutions were degassed under vacuum and filtered before use. Ultrapure water (Milli-Q-plus system, Millipore) was used for solutions, and in the different cleaning steps. The PEI, PSS, and PAH polyelectrolytes were dissolved in 25 mM Tris (pH 8) at concentrations of 5 mg/mL, whereas PLL was at a concentration 1 mg/mL. GlcNac was used at a 0.00125 mM concentration, in order to ensure a ratio of 1 molecule of GlcNac/10 molecules of rM179. PEM's were built up by sequential deposition of PSS and PAH from their solutions onto a precursor layer of PEI and all adsorption steps were separated by rinsing.

2. *Protein.* Recombinant mouse amelogenin (rM179) was expressed in *E. coli*, purified using a cation exchange and a reversed phase HPLC column and characterized as previously described.<sup>33</sup> GlcNac binding motif of rM179 is located in the 13-residue tyrosyl C-terminal domain (bold sequence below):

PLPPHPGSPGYINLSYEVLTPKWKYQSMIR**PYPSYGYEP-**  
**MGGWLHHQIIPVLSQQHPPSHTLQPHHPLPVVPAQQPVA-**  
**PQQPMMPVPGHHSMTPTQHHQPNIPPSAQPPFQQPFQ-**  
**PQAIPPQSHQPMQPSPLHPMQLAPQPPLPLFSMQPL-**  
**SPILPELPLEAWPATDKTKREEVD.**

rM179 was dissolved in 25 mM Tris (pH 8) at 0.25 mg/mL concentration. This pH and ionic strength assured a monodispersed population of the nanospheres. Acetonitrile, ACN 60% was added to the solution, when protein was kept in its monomeric form. Protein adsorption experiments were always made with freshly prepared suspensions. Temperature was carefully monitored during the measurements and kept at 24 or 37 °C, respectively, as specified in the Results section.

## Methods

**Streaming Potential Measurements.** Streaming potential measurements were carried out to determine the  $\zeta$  potential of the rM179 nanospheres. The experiments were performed on a homemade apparatus developed according to the method of Zembala and Déjardin.<sup>34</sup> The streaming potential is due to the flux of the buffer solution through an electrophoresis capillary (made from a fused silica tube) by applying an elevated N<sub>2</sub> pressure to a flask directly connected to the capillary. One measures the pressure and the potential differences on both sides of this 530  $\mu$ m narrow capillary via two flasks, each containing two Ag/AgCl electrodes. The  $\zeta$  potential is related to the pressure difference and to the streaming potential (difference in the potential measured on the two electrodes) by the Smoluchovski relation.<sup>35</sup>

In the experiments, first the streaming potential of the bare capillary filled with 25 mM Tris buffer (pH8) was measured. A 10 mL sample of 0.25 mg/mL concentrated rM179 solution was then injected with a syringe. The protein solution was kept

in the capillary for several hours, allowing it to adsorb to the capillary walls. The capillary was then extensively rinsed and equilibrated by the injection of 50 mL of Tris buffer and the streaming potential was subsequently measured.

**Optical Waveguide Light-Mode Spectroscopy (OWLS).** The buildup of polyelectrolyte multilayers (PEM) and protein adsorption onto PEM's were followed in situ by optical waveguide light-mode spectroscopy (OWLS).

OWLS is an optical technique based on the confinement of light in a high refractive index layer.<sup>36</sup> The core of the home-built experimental setup is an input grating sensor. This type of sensor makes use of the well-defined angle at which light couples into a waveguide by means of a grating coupler. The in-coupling equation gives the relation between certain discrete values of the  $\theta_i$  angle between the laser beam and the normal to the grating and the effective refractive index  $N$  of the whole system:

$$N = \sin \theta_i + l\lambda/\Lambda \quad (1)$$

where  $l$  represents the diffraction order, equal to 1 in our experimental condition,  $\lambda$  corresponds to the wavelength of the light, and  $\Lambda$  is the grating constant.

On the high index film of a waveguide covered by the solution present in the cell, an adlayer is adsorbed in the first step. In consecutive steps the adsorption of additional adlayers of different materials is also possible. The changes of optical parameters in the cover, e.g., the thickness and refractive index of an adsorbed polyelectrolyte or protein adlayer, perturbs the evanescent field and leads to changes of the guided modes, highly sensitive for the changes of the effective refractive indices of the transverse electric and transverse magnetic modes ( $N_{TE}$  and  $N_{TM}$ ). By measuring the two modes simultaneously (p-polarized and s-polarized), the thickness and the refractive index of the adsorbed layer, assumed to be homogeneous, and isotropic can be calculated.

In our home-built apparatus, the waveguide is introduced in its holder and connected to three sealed cover holes (injection port, buffer entrance port, and buffer exit port tubes). The measuring cell has an internal volume of 37  $\mu\text{L}$  that makes this equipment, in terms of needed quantity, quite suitable for costly protein preparations. Buffer is flushed through the cell at a constant flow rate. The sample holder is thermostated and the temperature is recorded by a sensor embedded in the waveguide holder with a precision of 0.1  $^{\circ}\text{C}$ .

After reaching a stable baseline with the buffer flowing through the cell, the buildup of the polyelectrolyte multilayers film was performed as follows:

(i) The buffer flow is stopped and 100  $\mu\text{L}$  of the PEI solution was injected into the cell. As a result,  $N_{TE}$  and  $N_{TM}$  values increased and reached a plateau after about 10 min. When a stable adsorption signal was obtained, the buffer flow is restarted for 15–20 min to rinse the excess PEI from the cell.

(ii) In the same way, negatively charged PSS and positively charged PAH were alternatively adsorbed onto the waveguide. Thus, progressively PEI-PSS, PEI-(PSS-PAH)<sub>1</sub>, PEI-(PSS-PAH)<sub>1</sub>-PSS, ... layers were deposited. The adlayer obtained after the deposition of the  $n$ th pair of layers is noted PEI-(PSS-PAH) <sub>$n$</sub> . Onto such multilayered films, proteins can be further adsorbed. A regular buildup regime of the (PSS-PAH) <sub>$n$</sub>  multilayer is reached after at least three bilayers;<sup>37</sup> therefore, a PEM film constituted by four bilayers of PSS-PAH was always used. rM179 (0.25 mg/mL in 25 mM Tris, pH8) was then adsorbed onto the positively ending PEI-(PSS-PAH)<sub>4</sub> multilayer film. At these experimental conditions rM179 self-assembles to nano-

spheres. Therefore, depending on the experiment, during the continuous flow (4 mL/h) of the protein solution amelogenin nanospheres were in contact with the PEM surface, from 80 to 160 min. For comparison, rM179 adsorption was also performed by consecutive injections of 100  $\mu\text{L}$  protein solutions into the measuring cell, and the same kinetics of nanospheres adsorption was recorded (data not shown). Once the optical signals leveled off, the protein solution was replaced by buffer solution and the desorption of the proteins (if any) was monitored. To build multilayers from the negatively charged amelogenin nanospheres, PLL as a positively charged polyelectrolyte was adsorbed between the nanosphere adsorption steps, until a PEI-(PSS-PAH)<sub>4</sub>-(rM179-PLL)<sub>4</sub> mixed polyelectrolyte/nanosphere architecture was obtained. In other experiments the effect of GlcNAc was studied: GlcNAc was first adsorbed onto the top of the PEI-(PSS-PAH)<sub>4</sub> film, followed by nanosphere adsorption, until, in theory, a PEI-(PSS-PAH)<sub>4</sub>-(GlcNAc-rM179)<sub>2</sub> architecture was obtained. When adsorption of rM179 monomers was monitored, the solution contained ACN 60%. All our experiments were performed in a liquid cell, the PEMs were built up from aqueous solutions. Earlier Scanning Angle Reflectometry measurements on PSS-PAH wet films were successfully analyzed by the optical invariants method and evidenced that these layers can be considered homogeneous and isotropic.<sup>38–40</sup> Therefore, OWLS data were analyzed by assuming that the polyelectrolyte multilayers behave as homogeneous and isotropic films. To the contrary, an optical anisotropy was reported in dried PEM films.<sup>51</sup> The additionally adsorbed proteins were then analyzed assuming a homogeneous, isotropic bilayer system. The details of the data analysis were previously described.<sup>38,39</sup>

The measured  $N_{TE}$  and  $N_{TM}$  values depend on the refractive index profile of the film deposited on the oxide layer. The mode equations were resolved with no thin layer approximation<sup>38,39</sup> and thus the structural parameters, i.e., refractive index and thickness ( $n_A$ ,  $d_A$ ) of each deposited layer were obtained. The surface mass density, expressed in  $\mu\text{g}\cdot\text{cm}^{-2}$  can be then calculated from the relation

$$\Gamma = (dn/dc)^{-1}(n_A - n_C)d_A \quad (2)$$

where,  $dn/dc$  is the refractive index increment of the protein solution and  $n_C$  is the refractive index of the cover solution. The refractive index increment of the protein was 0.18  $\text{cm}^3\cdot\text{g}^{-1}$ , as stated for numerous proteins.<sup>42</sup> For the polyelectrolytes, the values of 0.237 and 0.225  $\text{cm}^3\cdot\text{g}^{-1}$  were used for PSS and PAH, respectively.

**Fourier Transform Infrared Spectroscopy (FTIR).** Fourier transform infrared spectroscopy in attenuated total reflection mode (FTIR-ATR) was employed to check conformational changes in rM179 induced by the adsorption process. FTIR-ATR spectra were measured with an Equinox 55 spectrophotometer (BRUKER) on the surface of a ZnSe crystal using a liquid nitrogen-cooled MCT detector. Single channel spectra from 512 interferograms were calculated between 4000 and 400  $\text{cm}^{-1}$  with 2  $\text{cm}^{-1}$  resolution using Blackman-Harris three-term apodization and the standard Bruker OPUS/IR Software (Version 3.0.4). The analysis of the infrared spectra was carried out using the SPSErv software.<sup>29</sup> The FTIR experiments were performed in deuterated 25 mM TRIS buffer. The spectra of the precursor PEI-(PSS-PAH)<sub>4</sub> multilayer film deposited onto the ZnSe crystal was first recorded. The experimental conditions were the same as for OWLS. Then the recombinant mouse amelogenin (rM179) was adsorbed onto the film from a 0.25 mg/mL solution at pD 8.0 (the 0.4 unit shift between pH and



pD was taken into account). The protein solution was circulated with a peristaltic pump above the ZnSe crystal until protein adsorption reached saturation. The progress of the adsorption was monitored via recording FTIR spectra. To remove non- or weakly bound substances, washing with pure buffer separated the adsorption steps. In certain experiments, the first protein layer was covered with GlcNac, and then a second protein layer was added. These measurements furnished structural data on the protein nanospheres. The same experiments were performed in the presence of ACN 60% in order to monitor conformational changes in the monomeric rM179.

## Results and Discussion

**The  $\zeta$  Potential of rM179 Nanospheres and Their Adsorption on Charged Surfaces.** The adsorption of amelogenin onto silica was followed first by streaming potential measurement. Initially the bulk capillary had a  $\zeta$  potential of  $-72.8$  mV. Flowing in the solution of rM179 (0.25 mg/mL in 25 mM TRIS, pH 8), the  $\zeta$  potential decreased to  $-33.6$  mV. This value measured after a thorough washing of the capillary with buffer, shows that nanospheres were irreversibly adsorbed on the surface, however they were slightly negatively charged.

Since it turned out that rM179 nanospheres have a negative  $\zeta$  potential, we further studied their adsorption on a surface previously coated with a positively ending PEI-(PSS-PAH)<sub>4</sub> PEM. The film build-up and the amelogenin adsorption at 24 °C were monitored in situ by OWLS. The recorded increases in the effective refractive index of the transverse electric mode ( $N_{TE}$ ) versus time (Figure 1A.) indicate the step by step buildup of the PEI-(PSS-PAH)<sub>4</sub> film onto the planar waveguide, and the following adsorption of rM179 nanospheres. The amount of adsorbed material was calculated and the layer-by-layer increase of the adsorbed amount is shown in Figure 1B. Data points represent averages of four experiments. The well-known linear growth regime of the precursor PEM film is followed by an important amount of adsorbed rM179 nanospheres:  $\Gamma = 1.88 \pm 0.32 \mu\text{g}/\text{cm}^2$ . Coating surfaces by polyelectrolyte films proves to be a useful tool to immobilize this kind of nanostructures formed by strongly hydrophobic proteins.

Calculation of the thickness of the adsorbed layer, at 24 °C revealed decrease of the adsorbed nanospheres from a  $54 \text{ nm} \pm 2.3$  thick layer to  $26.4 \text{ nm} \pm 2.3$  following rinsing. That is the layer formed by the irreversibly adsorbed rM179 nanospheres. Earlier results have already shown the formation of thick protein layers extending up to several times the largest dimension of the protein when the protein and the surface are oppositely charged.<sup>40,43</sup> The authors reported on the formation of thick layers up to 48 nm when human serum albumin was adsorbed on PAH ending PEM's.<sup>40</sup> In our case the behavior of the adsorption kinetic suggests that after rinsing with pure buffer there is one stable monolayer of nanospheres that stays irreversibly bound to the surface. Considering one monolayer, its thickness has the dimension of the nanospheres in solution indicating that rM179 self-assembly is not disturbed when adsorbed on surfaces. When performed at 37 °C, the OWLS data (Figure 2A) showed that significantly thicker nanosphere layers of  $60.0 \pm 7.0$  nm were formed, than at 24 °C, corresponding to the previously observed temperature induced variations in rM179 nanospheres diameter in solution.<sup>1,6</sup> When the rM179 nanosphere layer adsorbed originally at 37 °C was rinsed with a buffer at 24 °C (Figure 2B), the obtained final thickness was about  $24.0 \pm 4.4$  nm, indicating, that even in adsorbed form the nanospheres were capable of undergoing

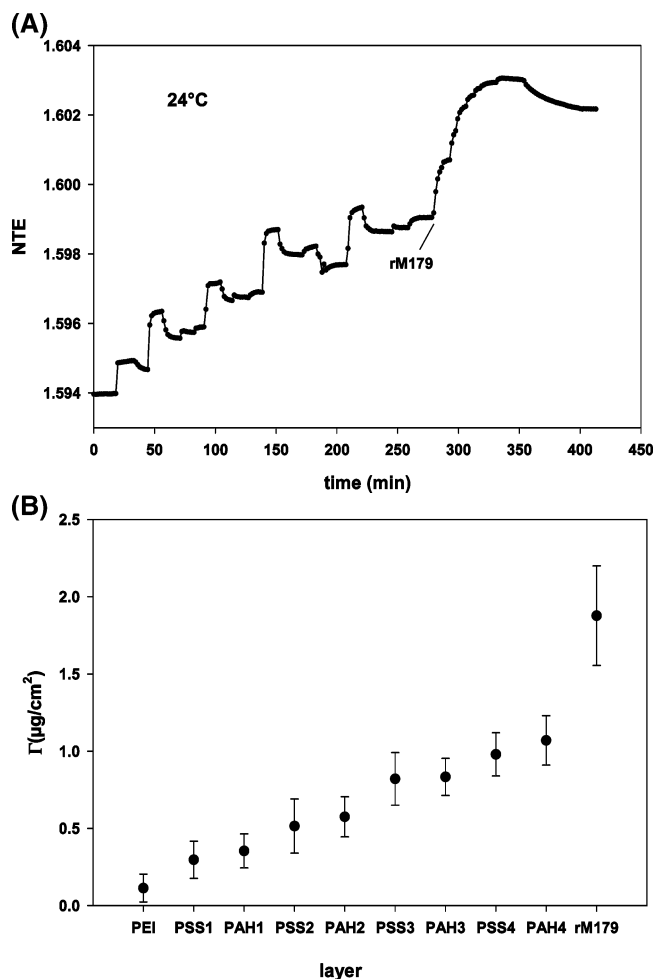


**Figure 1.** (A) Changes of the effective refractive index of the transverse electric mode ( $N_{TE}$ ) upon buildup of PEI-(PSS-PAH)<sub>4</sub> film followed by adsorption of rM179 at 24 °C. (B) Typical layer-by-layer buildup of the PEI-(PSS-PAH)<sub>4</sub>-rM179 matrix expressed by the calculated adsorbed quantities. The PEI, PSS, and PAH polyelectrolytes were adsorbed from a 5 mg/mL solution in 25 mM Tris (pH 8); rM179 was also dissolved in 25 mM Tris (pH 8) at 0.25 mg/mL concentration.

temperature induced size- variations. Seemingly, the contacts required for remaining adsorbed on the polyelectrolyte film surface do not disturb the intermolecular interactions, which maintain the amelogenin nanospheres.

The adsorption kinetics and the temperature-induced variations as analyzed by OWLS strongly suggest that a monolayer of nanospheres is adsorbed in an irreversible way onto the positively ending PEM. Adsorption of rM179 nanospheres reveal slow kinetics of about 100 min at 24 °C and 200 min at 37 °C and hardly reaching saturation, as if the spheres could deposit one on each other. These loosely bound structures however are removed with rinsing, since subsequently it returns to the thickness of a monolayer of spheres, irreversibly adsorbed on the surface. Once a layer of nanospheres is formed, the adsorption process ends and no second layer could be irreversibly added.

The observed slower adsorption kinetics at higher temperatures is rather surprising, but one should consider that at 37 °C the nanospheres are three times bigger than at 24 °C. When arriving close to the surface, a rearrangement of these nanospheres may also take place slowing down the adsorption kinetics. Some aspects of amelogenin nanospheres behavior can be compared to the superspheres described by Ramsden.<sup>44</sup> The

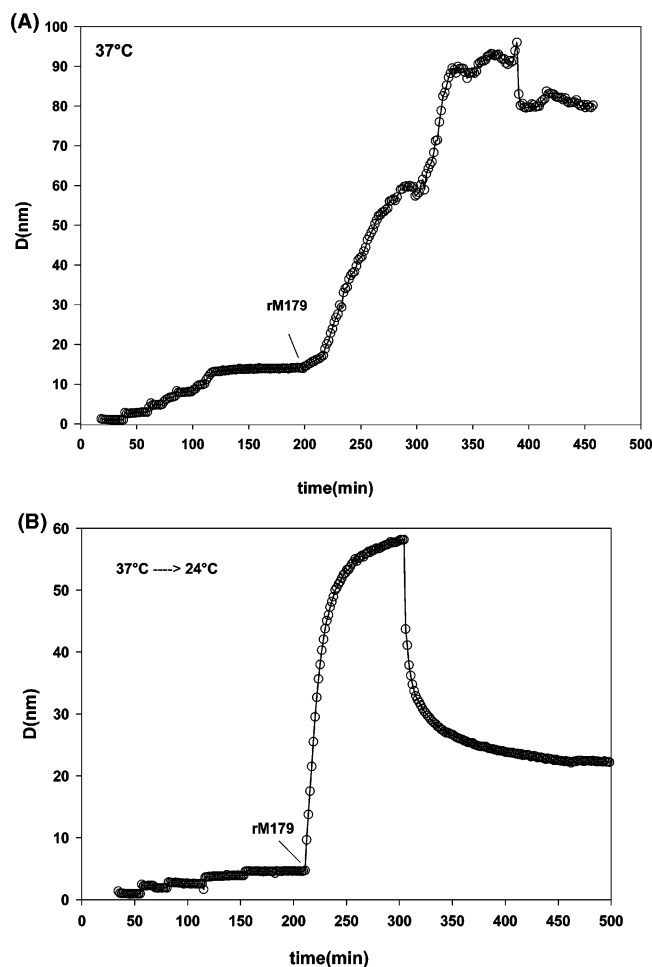


**Figure 2.** Adsorption kinetics expressed by the thickness of the adsorbed rM179 nanospheres on a precursor PEI-(PSS-PAH)<sub>4</sub> film at (A) 37 °C and (B) at 37 °C, but followed by a rinsing step at 24 °C. The polyelectrolyte and protein solutions were prepared in the same conditions as for Figure 1.

stability of superspheres with a negative external charge was explained by the balance of two opposing forces: the long-range electrostatic repulsion and the short-range attractive dispersion. In the case of amelogenin nanospheres, the existence of negative external charge that might stabilize the nanospheres has been already reported.<sup>4</sup> The superspheres theory considers aggregation of solid and inorganic particles, whereas amelogenin is a flexible macromolecule. When considering the self-assembly of biological molecules some other chemical forces relating to conformational changes and hydrophobic interactions will be also involved.

**Multilayers of Amelogenin Nanospheres as Mediated by poly-(L-Lysine).** Considering the observation that amelogenin nanospheres are slightly negative, we have attempted to build protein/polyelectrolyte architectures. We have succeeded in depositing on the top of a PEI-(PSS/PAH)<sub>4</sub> film a (rM179/PLL)<sub>4</sub> architecture where PLL is a cationic polyamino acid, poly(L-lysine). The recorded  $N_{TE}$  values show significant rM179 adsorption when mediated by PLL, which itself produces a relatively small signal increase (Figure 3A). The adsorption kinetics of the rM179 nanospheres on PLL reveals a slow adsorption process that seems to never reach saturation. The optical signal continues to increase after 60, or even 150 min (second rM179 layer), indicating continuous protein deposition, but the loosely attached rM179 nanospheres were always removed by the successive rinsing step. The calculated thicknesses of the layers are in the range of 11–15 nm (Figure 3B);

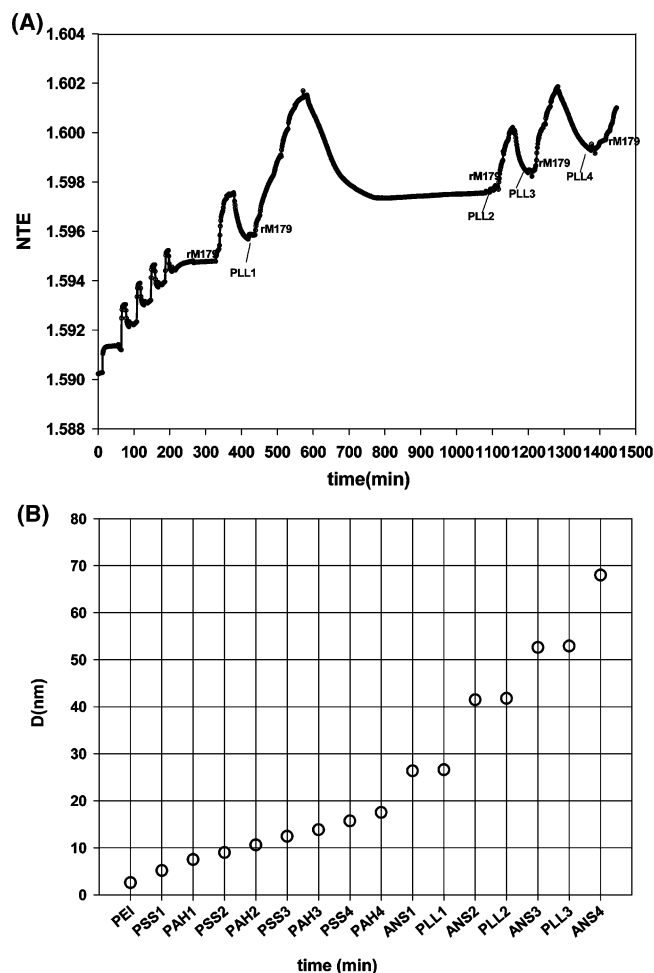


**Figure 3.** (A) Raw  $N_{TE}$  data signal obtained during the in situ buildup of a (rM179-PLL)<sub>4</sub> nanosphere multiassembly on a precursor film of PEI-(PSS-PAH)<sub>4</sub>. (B) Evolution of the calculated thicknesses for the finally obtained PEI-(PSS-PAH)<sub>4</sub>-(rM179-PLL)<sub>4</sub> matrix. Both the polyelectrolytes and protein were dissolved in 25 mM Tris (pH 8), at a concentration of 5 mg/mL for PEI, PSS, PAH, 1 mg/mL for PLL and 0.25 mg/mL for the rM179.

thus, they are thinner than the thickness of the monolayers presented in Figures 1 and 2.

The slight difference might originate in the different protein batch we used in the two sets of experiments. However, considering the obtained layer thicknesses, which are very close to each other, we can state, that a four-layered matrix of rM179 nanospheres was successfully built up by means of a charge driven (positive PLL) layer-by-layer adsorption process. This mixed protein/polyelectrolyte architecture remained stable for at least 2 days highlighting the potential of this system for possible medical applications.

**Formation of Multilayers of Amelogenin Nanospheres Mediated by GlcNAc.** Since positive PLL-mediated assembling of nanospheres was possible, we were interested to study whether the cationic N-acetyl-D-glucosamine (GlcNAc), known to specifically bind to the three-tyrosil motif in amelogenins (see bold sequence in Materials and Methods) will have similar effect. These studies allowed us to gather some information on the nature of interactions between the rM179 nanospheres and cationic GlcNAc, but also to learn on the driving forces of sequential layering by comparing the two multilayered systems: PLL and GlcNAc mediated nanospheres that proved to reveal important differences. Figure 4A,B shows the formation of a first, 13 nm thick monolayer of rM179 nanospheres on the

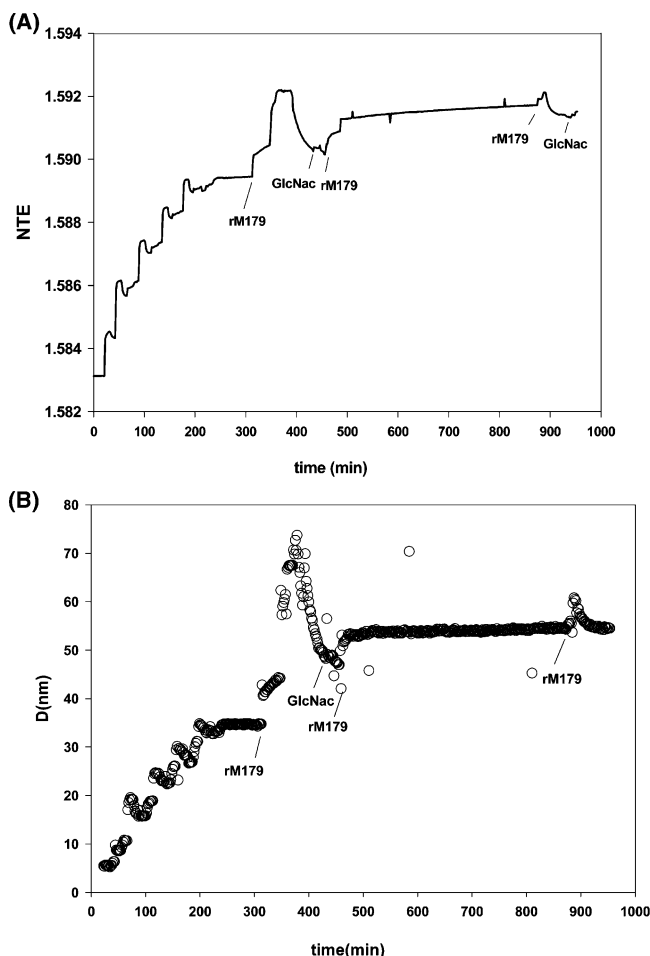


**Figure 4.** Adsorption kinetics of GlcNac mediated rM179 nanosphere adsorption on a precursor PEI-(PSS-PAH)<sub>4</sub> film in situ monitored by the changes in the effective refractive index  $N_{TE}$  (A). (B) The calculated thickness values reveal that multilayering nanospheres by means of GlcNac gradually ends. The experimental conditions were the same as for the Figure 3; GlcNac was used at a 0.00125 mM concentration, in order to ensure a ratio of 1 molecule of GlcNac/10 molecules of rM179.

top of the PEI-(PSS-PAH)<sub>4</sub> multilayered film. This thickness is in good agreement with the nanosphere monolayer thicknesses obtained in the PLL-mediated nanosphere multilayer experiment (11–15 nm), since these rM179 samples came from the same batch. Adding GlcNac to the nanosphere layer decreased the thickness of the film.

The following adsorption step of amelogenin increased the film thickness by 7 nm, which is considerably smaller than the 13 nm found for the nanospheres. Waiting for a long time, there is a very slight continuous increase of the adsorbed amelogenin, and after a second injection of rM179, which caused only a transient increase in the adsorption, this loosely bound population disappears from the film surface (Figure 4). This phenomenon may indicate that the GlcNac-amelogenin interaction is stronger than amelogenin–amelogenin interactions for nanosphere formation. GlcNac is providing a positively charged “cover” on the top of the previously adsorbed amelogenin nanosphere monolayer. Then, due to the preferred interactions, only amelogenin-monomers adsorb in one layer onto the GlcNac-terminated film surface. The evidence that GlcNac inhibits the sequential charged adsorption of amelogenin onto polyelectrolyte multilayer film raises important questions about the nature of interactions between amelogenin (negatively charged) and GlcNac (positively charged) and support the

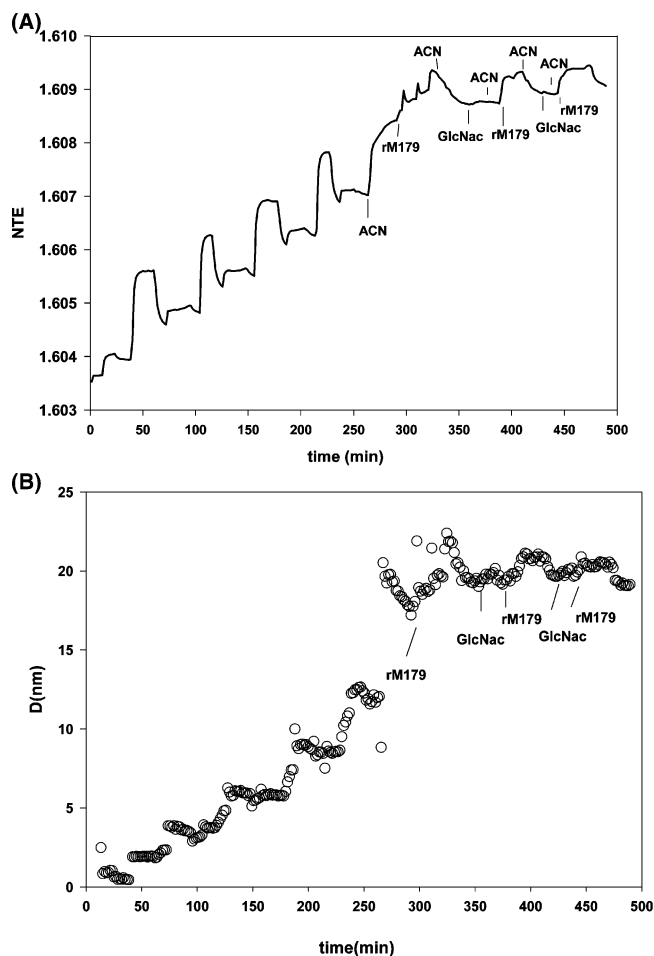


**Figure 5.** Layer-by-layer GlcNac mediated adsorption of rM179 monomers on a precursor PEI-(PSS-PAH)<sub>4</sub> film (A) monitored by  $N_{TE}$  and (B) the corresponding thickness. Polyelectrolytes were prepared as for the other experiments. rM179 was dissolved in 60% ACN at 0.25 mg/mL concentration. For a better insight the intermediate rinsing steps (with ACN) were pointed at on the figure.

possibility of electrostatic interactions between the two. It is noteworthy that addition of GlcNac to rM179 solution did not affect the particle size distribution as analyzed by dynamic light scattering (data not shown). This supports the idea that the hydrophobic interactions necessary for amelogenin assembly are not hindered following GlcNac addition or their molecules are simply not large enough to affect the size of amelogenin assemblies.

#### Adsorption of Monomeric rM179 on Charged Surfaces.

In order to investigate the role of the rM179 monomers in the adsorption processes, the same OWLS experiments were performed in the presence of acetonitrile (ACN) known to stabilize amelogenin monomers.<sup>4</sup> The raw  $N_{TE}$  data (Figure 5A) show the buildup of a PEM, the same as in the other experiments: PEI-(PSS-PAH)<sub>4</sub>, which is followed by an abrupt effective refractive index change. This is due to the injection of the ACN solution, that has a different refractive index ( $n = 1.44$ ) as compared with that of the polyelectrolyte solution ( $n = 1.335$ ) as measured with an Abbe refractometer. The signal growth after the successive injection of rM179 corresponds to the adsorption of a monolayer of monomeric amelogenin. The small peaks in the kinetic adsorption are the signatures of the successive injections of rM179 (Figure 5). Despite the originally large signal increase seen after washing with ACN, only a small part of rM179 stays irreversibly adsorbed.

The calculations reveal the formation of a protein layer of about 2 nm (Figure 5B.), suggesting that the protein can fully cover the adsorption surface which never extends over the monolayer, just as for the nanospheres. In terms of adsorbed quantity this corresponds to  $0.25 \mu\text{g}/\text{cm}^2$  adsorbed rM179.

In the next step, GlcNac was flushed onto the protein layer and, when reinjected, rM179 monomers readsorb again. Finally a GlcNac mediated assembly of three monolayers of rM179 monomers was obtained. We cannot predict from these measurements whether the multilayering is due to the interaction of GlcNac with the three tyrosyl motif in amelogenin, or there is just an electrostatic attraction between the negatively charged protein and positively charged GlcNac, or eventually the combination of two. However, we can underline the role of the latter in limiting the formation of protein layers exceeding one monolayer. The obtained results corroborate earlier published observations on the affinity of amelogenin for the GlcNac.<sup>45,46</sup>

Our OWLS data reveal that monomeric and auto-assembled amelogenin always form monolayers when adsorbed on PEM coated surfaces. When GlcNac was added, only rM179 monomers, and not the nanospheres could be deposited in several layers. Formation of multilayers of nanospheres was however possible when mediated by the cationic PLL.

**FTIR-ATR.** Generally, assembling is governed by the conformational states of molecules, therefore for a better insight we performed FTIR spectroscopy in attenuated total reflection mode.

The secondary structures of amelogenin, adsorbed among different conditions onto the polyelectrolyte film were determined from the spectra shown in Figure 6 by fitting Lorentzian-shaped component bands to the  $1700\text{--}1600 \text{ cm}^{-1}$  region of the FTIR spectra. The results of the fits are given in Table 1 for both the monomeric protein and its nanospheres. As it was previously reported, the presence of  $\beta$ -sheets and turns were evidenced<sup>47</sup> (Table 1).

However, according to the data in Table 1, there is a large difference between the secondary structure of the monomeric and the nanosphere-assembled forms of rM179 indicating conformational changes during nanosphere assembly. In the monomers, the amount of  $\alpha$ -helix is substantial but it is almost absent in the nanospheres. The total amount of  $\beta$ -structures observed in monomeric form was 47%, and this amount increased to 70% in the assembled amelogenin. The adsorption of GlcNac onto the surface of the protein-covered polyelectrolyte film excludes some of the earlier adsorbed protein from the surface (Figure 6.).

The structure of this protein fraction cannot be well determined in terms of the known secondary structure elements as indicated by the enormous errors ("GlcNac effect" column in Table 1). Since what we see is the total change of the whole polyelectrolyte film plus the adsorbed protein upon the GlcNac addition, the observed difference should not necessarily be the spectrum of the leaving amelogenin only. Thus, there must be other structural rearrangements in the polyelectrolyte + protein architecture than just the loss of a fraction of the adsorbed amelogenin. Probably because of the same reasons, the structure of the rM179 adsorbed in small amounts onto the GlcNac-treated nanosphere surface cannot be precisely determined either (Adsorption after GlcNac column in Table 1). The structure of the total protein, however, on the surface of the film after the GlcNac treatment is remarkably similar to that of the nanospheres. That is, the structure of the "perfect" nanospheres resists GlcNac; only peripheral rM179 proteins could be removed by GlcNac. Nanospheres, i.e., assembled amelogenins, could not

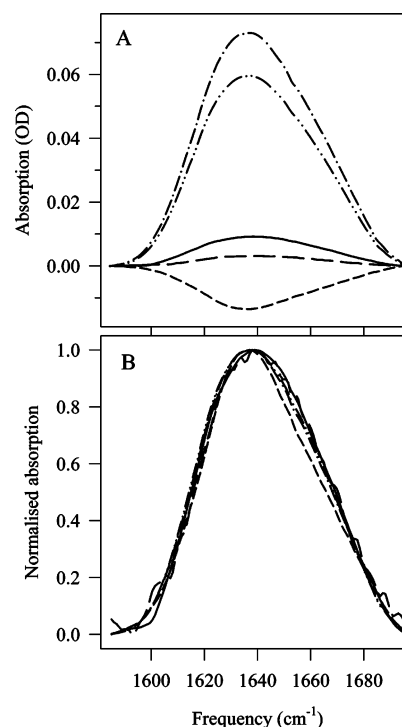


**Figure 6.** The amide I regions of ATR-FTIR absorption spectra of rM179 adsorbed onto a PEI-(PSS-PAH)<sub>4</sub> film among different conditions: (—) monomer, in the presence of 60% ACNi in D<sub>2</sub>O; (---) ThinSpaceEnDash nanosphere, rM179 adsorbed onto the same PEI-(PSS-PAH)<sub>4</sub> film obtained by alternated build-up of in D<sub>2</sub>O-based 25 mM TRIS buffer; (· · · ·) GlcNac effect, the film was treated with GlcNac, and as a result, some protein left the architecture; (— · —) adsorption after GlcNac, after the adsorption of 0.0125 mM GlcNac onto PEI-(PSS-PAH)<sub>4</sub>-rM179, rM179 was for the second time adsorbed among the same conditions as before; (— · · ThinSpace · ThinSpaceEnDash) total after GlcNac, the absorption spectrum of rM179, which remained in the film after the GlcNac treatment. Panel A: The original absorption spectra after a linear baseline subtraction between 1600 and  $1700 \text{ cm}^{-1}$ . Panel B: the normalized absorption spectra. Note, that here the GlcNac effect spectrum is multiplied with (−1) for better comparison with amide I band shapes.

adsorb onto the GlcNac-treated surface; only a layer of monomer-like amelogenin could be observed having altered secondary structure (Figure 6, Table 1). This would mean that GlcNac could alter considerably the secondary structure of only those proteins which arrive at the surface after its adsorption. This would also mean that different sites of the amelogenin molecules take part in binding GlcNac onto the nanospheres and in binding amelogenin (monomers) onto a (nanosphere/GlcNac) surface.

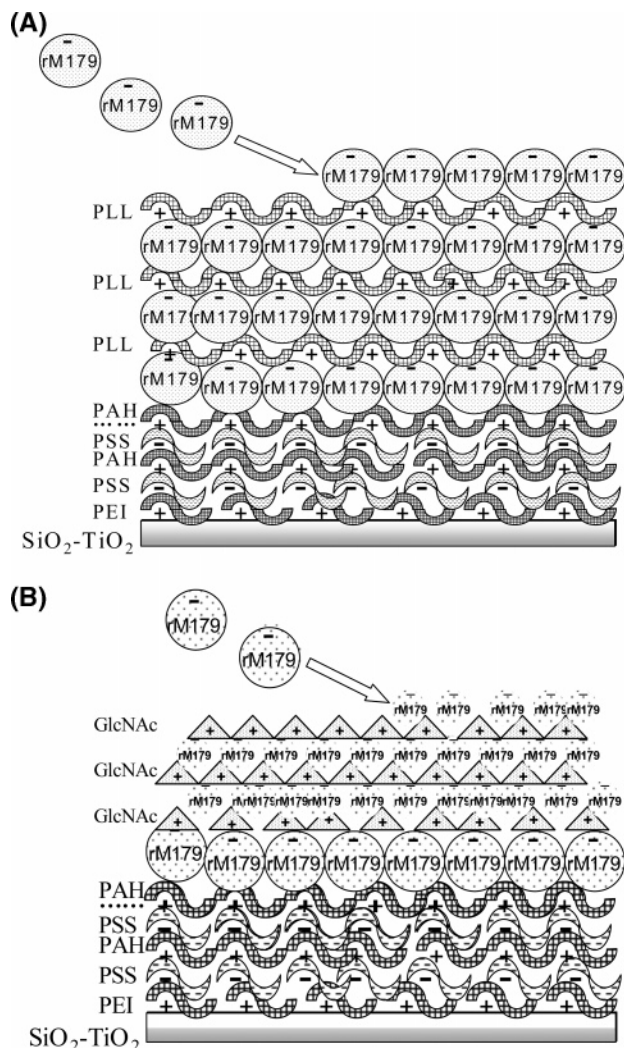
There is some discrepancy between the results obtained by CD and infrared spectroscopy concerning the secondary structure of amelogenin. While several CD measurements indicate the possible existence of polyproline II helices in the protein, there are infrared studies reporting a considerable band at around  $1625 \text{ cm}^{-1}$  in the amide I region.<sup>48</sup> Using FTIR spectroscopy, mostly turns and different  $\beta$ -structures are mentioned.<sup>47,49</sup> The observed differences can emerge from the sampling, as our FTIR-ATR measurements concerned the adsorbed form of proteins, contrary to the earlier publications, where protein in solution form was addressed. This gives an added value for our FTIR studies, constituting the first report on the structure of amelogenin in adsorbed form. In good agreement with our results presented in this paper, Raman spectroscopy also shows mixed  $\alpha$  helix,  $\beta$ -turn, and  $\beta$ -sheet structures.<sup>50</sup>



**Table 1.** Secondary Structure Analysis of the rM179 Protein among Different Conditions Based on the Decomposition of Its Amide I' Region into Lorentzian-shaped Component Bands. Initial Parameters of the Fit Were Obtained as Described Earlier<sup>24</sup>

amide I' components	component frequencies (cm <sup>-1</sup> )	monomer (%) <sup>a</sup>	nanosphere (%)	GlcNac effect (%)	adsorption after GlcNac (%)	total protein after GlcNac (%)
$\beta$ -antiparallel	1623–1627	43 ( $\pm$ 6)	27 ( $\pm$ 6)	28 ( $\pm$ 67)	24 ( $\pm$ 18)	25 ( $\pm$ 5)
$\beta$ -parallel	1637–1641	4 ( $\pm$ 1)	43 ( $\pm$ 8)	43 ( $\pm$ 151)		40 ( $\pm$ 7)
$\alpha$ -helix	1649–1655	38 ( $\pm$ 11)			71 ( $\pm$ 51)	
turns	1661–1669	13 ( $\pm$ 5)	30 ( $\pm$ 3)	28 ( $\pm$ 188)	4 ( $\pm$ 6)	35 ( $\pm$ 3)

<sup>a</sup> There were two other bands at around 1611–1612 and 1676–1683 cm<sup>-1</sup>, but their contribution never exceeded 2%; thus, they were omitted. Note that the "turns" can be interpreted as "poly Pro II"  $\beta$ -turn,  $\beta$ -strand, or unordered structures.<sup>50,51</sup>

**Figure 7.** Schematic presentation of the layer-by-layer building-up process of the PEI-(PSS-PAH)<sub>4</sub> positively ending PEM (for simplicity just 2 bilayers were presented in the schema), (A) followed by PLL mediated adsorption of four monolayers of amelogenin nanospheres: (rM179-PLL)<sub>4</sub>. Experimental conditions were as for the Figure 3, (B) followed by GlcNac mediated adsorption of three monolayers of monomeric amelogenin. Experimental conditions were the same as those for Figure 4.

## Conclusions

The present investigation highlights that by means of charge driven adsorption we can manipulate immobilization of mainly hydrophobic proteins such as amelogenin in mono- or multilayers. Single monolayer of monomers or nanospheres of rM179, adsorbed irreversibly onto a positively charged PEM film surface. Successive adsorption of nanospheres was possible when mediated by cationic PLL adsorption. The cationic GlcNac did not have the same effect. When applied onto a terminating

nanosphere layer GlcNac did not disturb the nanosphere-assembled protein's structure, and only monomeric amelogenin could be adsorbed onto the GlcNac-terminated surface. The difference between the effects of PLL and GlcNac on PEM-protein architecture construction is illustrated in Figure 7. The buildup might be disturbed by an interaction between the GlcNac saccharide-like residue and the three-tyrosyl motif in amelogenin that may be exposed on the nanosphere surface.

Multilayering of monomeric rM179 was possible when mediated by GlcNac adsorption. Infrared spectroscopy revealed a large difference between the secondary structures of the monomeric or nanosphere-assembled rM179 amelogenins indicating conformational changes during nanosphere assembly. While there was a considerable amount of  $\alpha$ -helices in the monomers,  $\beta$ -turn and  $\beta$ -sheet structures dominated the assembled proteins.

Our work constitutes the first report on a controlled in vitro buildup of an rM179 nanosphere monolayer-based matrix. The results confirm that while electrostatic forces dominate protein/PEM interactions, amelogenin self-assembly is mostly stabilized by hydrophobic interactions. Support for hydrophobic interactions was evidenced by previous works: the disassembling of nanospheres at low pH (pH inhibits hydrophobic interactions) and stability of monomeric amelogenin in the presence of acetonitrile (a relatively hydrophobic solvent) were observed.<sup>4</sup>

The existence of hydrophobic interactions was revealed also by the amino acid content and the nature of amelogenin as well as by the studies on protein–protein interactions through the N-terminal region of rM179.<sup>7</sup>

Our results show that amelogenin nanospheres are stable even after their adsorption onto polyelectrolyte multilayers, corroborating that hydrophobic interactions play major roles in assembly, although involvement of other interactions for assembly cannot be ruled out.

The sequential adsorption process of the nanospheres by means of PLL may constitute an appropriate model for investigating the protein–protein and protein–mineral interactions in the enamel matrix.

**Acknowledgment.** The authors thank Dr. Liliana Szyk (Institute of Catalysis and Surface Chemistry Cracovie, Poland) for supporting this work with  $\zeta$  potential measurements, Dr. Cs. Bagyinka, Biological Research Center, Szeged, Hungary, for the SPSERV software, and Mr. Christopher Abbott for protein purification. This work was supported by the NIH-NIDCR DE015332-01 and DE013414 grants to J.M.O. and by a bilateral Franco-Hungarian grant (F-5/03) to B.Sz. and C.G.

## References and Notes

- (1) Fincham, A. G.; Moradian-Oldak, J.; Simmer, J. P. *J Struct. Biol.* **1999**, *30*, 270.
- (2) Bartlett, J. D.; Ganss, B.; Goldberg, M.; Moradian-Oldak, J.; Paine, M. L.; Snead, M. L.; Wen, X.; White, S. N.; Zhou, Y. L. *Curr. Top. Dev. Biol.* **2006**, *74*, 57.

- (3) Moradian-Oldak J. The emergence of nanospheres as structural components adopted by amelogenin. *Discovery! J. Dent. Res.*, in press.
- (4) Moradian-Oldak, J.; Simmer, J. P.; Lau, E. C.; Sarte, P. E.; Slavkin, H. C.; Fincham, A. G. *Biopolymers* **1994**, *34*, 1339.
- (5) Fincham, A. G.; Moradian-Oldak, J.; Simmer, J. P.; Sarte, P.; Lau, E. C.; Diekwisch, T.; Slavkin, H. C. *J Struct. Biol.* **1994**, *112*, 103.
- (6) Moradian-Oldak, J.; Tan, J.; Fincham, A. G. *Biopolymers* **1998a**, *46*, 225.
- (7) Moradian-Oldak, J.; Leung, W.; Fincham, A. G. *J. Struct. Biol.* **1998**, *122*, 320.
- (8) Aichmayer, B.; Margolis, H. C.; Sigel, R.; Yamakoshi, Y.; Simmer, J. P.; Fratzl, P. *J. Struct. Biol.* **2005**, *151*, 239.
- (9) Fincham, A. G.; Moradian-Oldak, J.; Diekwisch, T. G. H. *J. Struct. Biol.* **1995**, *115*, 50.
- (10) Moradian-Oldak, J.; Goldberg, M. *Cells Tiss. Org.* **2005**, *18*, 202.
- (11) Moradian-Oldak, J.; Bouropoulos, N.; Wang, L.; Gharakhanian, N. *Matrix Biol.* **2002**, *21*, 197.
- (12) Paine, M. L.; Snead, M. L. *J. Bone Miner. Res.* **1997**, *12*, 221.
- (13) Aoba, T.; Fukae, M.; Tanabe, T.; Shimizu, M.; Moreno, E. C. *Calcif. Tissue Int.* **1987**, *41*, 281.
- (14) Paine, M. L.; Lei, Y.-P.; Dickerson, K.; Snead, M. L. *J. Biol. Chem.* **2002**, *277*, 17112.
- (15) Moradian-Oldak, J.; Paine, M. L. Biomineralization. From Nature to Application. In *Metal Ions in Life Sciences*; Sigel, A., Sigel, H., Sigel, R. K. O., Eds.: John Wiley & Sons, Ltd., Chichester, U.K., in press; Vol. 4.
- (16) Du, C.; Falini, G.; Fermari, S.; Abbott, C.; Moradian-Oldak, J. *Science* **2005**, *307*, 1450, Erratum: *Science* **2005**, *309*, 2166.
- (17) Moradian-Oldak, J.; Du, C.; Falini, G. *Eur. J. Oral Sci.* **2006**, *114*, 289.
- (18) Fincham, A. G.; Moradian-Oldak, J.; Simmer, J. P. *J. Struct. Biol.* **1999**, *126*, 270.
- (19) Robinson, C.; Fuchs, P.; Weatherell, J. A. *J. Cryst. Growth* **1981**, *53*, 160.
- (20) Beniash, E.; Simmer, J. P.; Margolis, H. C. *J. Struct. Biol.* **2005**, *149*, 182.
- (21) Margolis, H. C.; Beniash, E.; Fowler, C. E. *J. Dent. Res.* **2006**, *85*, 775.
- (22) Grinnell, F.; Feld, M. K. *J. Biol. Chem.* **1982**, *257*, 4888.
- (23) Qiu, Q.; Sayer, M.; Kawaja, M.; Shen, X.; Davies, J. E. *J. Biomed. Mater. Res.* **1998**, *42*, 117.
- (24) Dufrene, Y. F.; Marchal, T. G.; Rouxhet, P. G. *Langmuir* **1999**, *15*, 2871.
- (25) Absolom, D. R.; Zing, W.; Neumann, A. W. *J. Biomed. Mater. Res.* **1987**, *21*, 161.
- (26) Norde, W.; Lyklema, J. *Biomater. Sci. Polym. Ed.* **1991**, *2*, 183.
- (27) Decher, G.; Hong, J. D.; Schmitt, J. *Thin Solid Films* **1992**, *210*, 831.
- (28) Caruso, F.; Mohwald, H. *J. Am. Chem. Soc.* **1999**, *121*, 6039.
- (29) Schwinté, P.; Voegel, J.-C.; Picart, C.; Haikel, Y.; Schaaf, P.; Szalontai, B. *J. Phys. Chem. B* **2001**, *105*, 11906.
- (30) Montrel, M. M.; Sukhorukov, G. B.; Petrov, A. I.; Shabarchina, L. I.; Sukhorukov, B. I. *Sens. Actuators, B* **1997**, *42*, 225.
- (31) Muller, M. *Biomacromolecules* **2001**, *2*, 262.
- (32) Decher, G. *Science* **1997**, *277*, 1232.
- (33) Simmer, J. P.; Lau, E. C.; Hu, C. C.; Bringas, P.; Santos, V.; Aoba, T.; Lacey, M.; Nelson, D.; Zeichner-David, M.; Snead, M. L.; Slavkin, H.; Fincham, A. G. *Calcif. Tissue Int.* **1994**, *54*, 312–319.
- (34) Zembala, M.; Déjardin, P. *Colloid Surf. B* **1994**, *3*, 119–129.
- (35) Hunter, R. J. *Zeta Potential in Colloid Science*; Academic Press: New York, 1981.
- (36) Tiefenthaler, K.; Lukosz, W. *J. Opt. Soc. Am., B* **1989**, *6*, 209.
- (37) Ladam, G.; Schaad, P.; Voegel, J.-C.; Schaaf, P.; Decher, G.; Cuisinier, F. J. G. *Langmuir* **2000**, *16*, 1249.
- (38) Picart, C.; Ladam, G.; Senger, B.; Voegel, J.-C.; Schaaf, P.; Cuisinier, F. J. G.; Gergely, C. *J. Chem. Phys.* **2001**, *115*, 1086.
- (39) Picart, C.; Gergely, C.; Senger, B.; Arntz, Y.; Voegel, J.-C.; Schaaf, P.; Cuisinier, F. J. G. *Biosens. Bioelectron.* **2004**, *20* (3), 553.
- (40) Ladam, G.; Gergely, C.; Senger, B.; Decher, G.; Voegel, J.-C.; Schaaf, P.; Cuisinier, F. J. G. *Biomacromolecules* **2000**, *1*, 674.
- (41) Ramsden, J. J.; Lvov, Yu. M.; Decher, G. *Thin solid films* **1995**, *254*, 246.
- (42) Feijter, J. A.; Benjamins, J.; Veer, F. A. *Biopolymers* **1978**, *17*, 1759.
- (43) Gergely, C.; Bahi, S.; Szalontai, B.; Flores, H.; Schaaf, P.; Voegel, J. C.; Cuisinier, F. J. G. *Langmuir* **2004**, *20*, 5575.
- (44) Ramsden, J. J. *Proc. R. Soc. London, Ser. A* **1987**, *413*, 407.
- (45) Ravindranath, R. M. H.; Moradian-Oldak, J.; Fincham, A. G. *J. Biol. Chem.* **1999**, *274*, 2464.
- (46) Ravindranath, R. M.; Tam, W. Y.; Pauline, N.; Fincham, A. G. *J. Biol. Chem.* **2000**, *275*, 39654.
- (47) Renugopalakrishnan, V.; Strawich, E. S.; Horowitz, P. M. Glimcher, M. J. *Biochemistry* **1986**, *25*, 4879.
- (48) Timasheff, S. N.; Susi, H.; Stevens, L. *J. Biol. Chem.* **1967**, *242*, 5467.
- (49) Jodaikin, A.; Weiner, S.; Perl-Treves, D.; Traub, W.; Termine, J. D. *Int. J. Biol. Macromol.* **1987**, *9*, 166.
- (50) Zheng, S. T.; Renugopalakrishnan, V.; Strawich, E.; Glimcher, M. J. *Biopolymers* **1987**, *26*, 1809.
- (51) Bochicchio, B.; Tamburro, A. M. *Chirality* **2002**, *14*, 782.

BM070088+